Melting of Normal Hydrogen Under High Pressures Between 20 and 300 Kelvins

Abstract. *The melting curve of normal hydrogen has been determined up to 52 kilobars between 20 and 300 Kelvins. The results are in excellent agreement with the modified Simon equation proposed for hydrogen below 19 kilobars, but not with the existing theoretical predictions. The results also provide an independent check on the validity of the ruby high-pressure scale at low temperature.*

In 1926, Bernal proposed that all matter subjected to high enough pressure should be metallic. The search for such a universal ultimate transformation of an insulator to a metal has become one of the most interesting problems in high-pressure science. Being the simplest element in the periodic table, molecular hydrogen is particularly attractive for the study. In addition, the attainment of a metallic phase of hydrogen (*1*) can be of important technological and astrophysical significance. Several calculations (*2*) have been made on the critical pressure of hydrogen above which the metallic phase is stabilized. The critical pressure is defined as the intersection pressure of the Gibbs' energy versus pressure curves of the molecular and metallic phases of hydrogen. It is, therefore, sensitive to the equations of state of both solid phases. The uncertainty in the equations of state at high pressure has been suggested as responsible for the large variation of the calculated critical pressure (*3*) from 0.25 to 20 Mbar. Since metallic hydrogen is probably similar to an alkaline metal whose equation of state is obtainable, the uncertainty is considered to arise mainly from the equation of state of the molecular phase, for which reliable experimental data above 25 kbar (static) do not exist. Using a newly developed cryogenic high-pressure press, we have determined the melting curve of normal hydrogen up to 52 kbar and 300 K. The results will provide an effective although indirect check on the intermolecular potential of hydrogen at high pressure, from which the equation of state is constructed and the thermodynamic properties are derived.

A beryllium-copper cryogenic press with a diamond anvil high-pressure cell (*4*) was constructed for this study. We could vary the pressure at low temperature by adjusting a pair of screws outside the cryostat. We were able to make in situ optical measurements, including direct visual observations, by mounting the objective of a specially designed telemicroscope on the top of the pressure cell. The telemicroscope serves as a conduit for both in and out optical signals. The sample chamber is a hole (200 μm in diameter) in a type 301 stainless steel gasket 250 μm thick confined between two diamond anvils housed inside the high-pressure cell. The sample temperature was controlled by a Manganin heater wrapped around the exterior wall of the cell. The press assembly is situated inside a liquid-helium cryostat. The pressure was determined by a ruby manometer (*5*) located within the sample chamber (with a resolution of ± 0.3 kbar) and the temperature by a chromel-alumel thermocouple situated next to the sample (with a resolution of ± 0.1 K). We loaded normal hydrogen at low temperature into the sample chamber by condensing 99.999 percent high-purity hydrogen gas at ~16 K. We then sealed the sample in the chamber by raising the lower piece of the diamond anvil set against the top piece.

The wavelength (λ) of the ruby R_1 fluorescence line was measured between 4.2 and 300 K. At 1 atm pressure, λ remains constant up to ~77 K and increases rapidly with further increase in temperature. The temperature-induced shift, Δλ, of λ between 77 and 300 K can be described by the expression (*6*)

$$1/\Delta\lambda(T) = \alpha(T/T_D)^4 \int_0^{T_D/T} [x^3/(e^x - 1)]dx$$

based on a two-phase Raman process, with the electron-phonon parameter $\alpha = -408\ cm^{-1}$ and the Debye temperature $T_D = 725$ K. The slightly different values of α and T_D from those reported earlier may be attributed to the different ruby crystals used. The pressure coefficient of λ has been measured between 4.2 and 358 K up to 12 kbar (*7*) and has been found to be the same as that at 300 K up to ~1.7 Mbar (*4*). We therefore determined the pressure experienced by the hydrogen sample in the present investigation by using the temperature-independent pressure coefficient of λ, 0.036 nm/kbar (*4*), and taking the temperature-induced shift of λ into consideration.

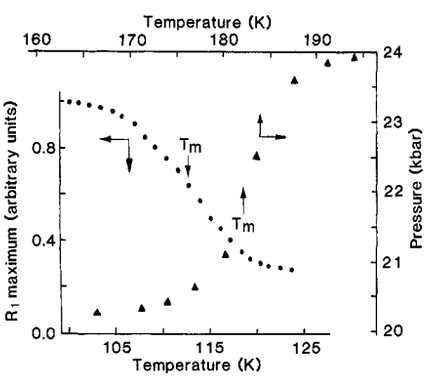

Fig. 1. The temperature dependence of pressure inside the sample chamber near T_m and the temperature dependence of the intensity of the R_1 line for a constant λ maximized away from T_m.

Usually, at a liquid-solid phase transition, enhanced diffused light scattering occurs because of the presence of a mixed phase region when the temperature excursion rate in traversing the transition is high, and a pressure shift inside the sample chamber occurs as a result of the volume difference between the two phases. One can thus determine the melting point of hydrogen as the temperature varies by three methods: method 1, by visually observing the intensity of the transmitted light through the sample; method 2, by measuring the pressure inside the sample chamber; or method 3, by continuously monitoring the intensity of the R_1 line, maximized at a fixed λ, away from the transition. The liquid-solid phase transition then manifests itself as a sudden drop in the transmitted light intensity (only at the transition), a sharp rise (drop) in pressure on warming (cooling), and a drastic drop in the intensity of the R_1 line. Typical results obtained by methods 2 and 3 are displayed in Fig. 1.

Although all three methods were used in determining the melting temperature (T_m), method 1 was used only on cooling when a high cooling rate of our cryogenic press was achievable and method 3 only below 150 K when the temperature-induced shift in λ is small. The uncertainty in T_m determined by method 1 can be rather large depending on the cooling rate, but that by other methods is small (± 0.5 K). The observed temperature hysteresis during melting, upon warming and cooling, was less than 3 K. The pressure in the liquid phase immediately above T_m was taken as the melting pressure (P_m) and should be hydrostatic. A plot of T_m versus P_m for two hydrogen samples is shown in Fig. 2. The uncertainties in T_m (± 0.5 K) and P_m (± 0.6 kbar) are smaller than those represented by the size of the data points. All data points were determined by more than one method, with method 2 being the primary method of detection, and were reproduced in several experiments. Although a pressure exceeding 150 kbar was easily obtained at low temperature (for example, < 77 K), leakage developed

0036-8075/81/0619-1393$00.50/0 Copyright © 1981 AAAS

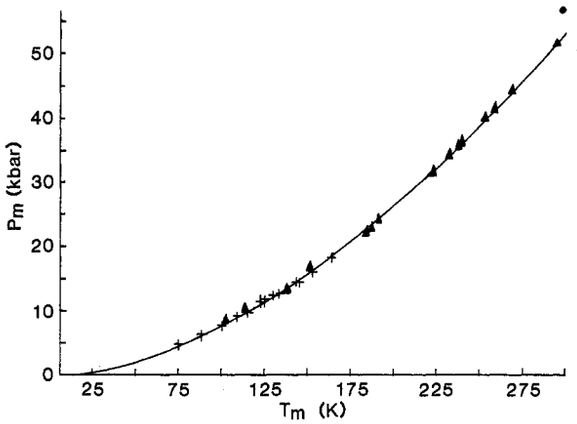

Fig. 2. A plot of P_m versus T_m for normal hydrogen: ▲, present work; x, from (*8*); ●, from (*9*); and the solid curve–modified Simon equation from (*8*).

in the sample chamber after repeated temperature and pressure cyclings above 300 K.

The melting curve of normal hydrogen was determined up to 19 kbar by Liebenberg *et al.* (*8*), using a piston-cylinder apparatus such that the absolute pressure could be measured. A modified Simon melting equation (where P_m has the dimension kilobars)

$$P_m = -0.2442 + 2.858 \times 10^{-3} T_m^{1.724}$$

was proposed as a least-squares fit to their data. The same equation describes our results well and is shown as a solid curve in Fig. 2; results obtained by Liebenberg *et al.* are shown for comparison. The surprisingly good agreement between the modified Simon equation proposed by Liebenberg *et al.* and our results suggests that the ruby pressure scale is an absolute scale, at least below 175 K. Mao and Bell (*9*) reported a P_m of 57 kbar at 298 K, in contrast to the 53 kbar from this investigation. It should be noted that the intense laser beam used to excite the ruby fluorescence can drastically enhance the local temperature of the sample and thus can introduce a significant error to T_m, particularly when method 1 is used. In our experiment, the laser power was kept as low as possible (*10*).

Ross (*11*) has calculated P_m based on an effective pair potential obtained from analyzing the shock compression data at high pressure and temperature. The value of P_m so calculated was 78 kbar at 250 K, in contrast to 39 kbar from our study. The large disagreement may be attributed to the basic difference of hydrogen (*1*) at low (a quantum solid) and high (a classical solid) temperatures or to the difference in pressure scales at high and low pressure. Grigorev *et al.* (*12*), using an equation of state in the Mie-Grüneisen form with experimentally determined parameters, showed that a value of 41 kbar could be predicted for P_m at the same temperature. The disagreement with our value is small but exceeds the experimental uncertainty. Since the equation of state was an empirical one, the disagreement may be ascribed to the difference in pressure scales.

V. DIATSCHENKO
C. W. CHU

Department of Physics and
Energy Laboratory,
University of Houston,
Houston, Texas 77004

References and Notes

1. M. Ross and C. Shishkevish, *Molecular and Metallic Hydrogen* (Report R-2056-ARPA, Rand Corporation, Santa Monica, Calif., May 1977).
2. A. K. McMahan, *High Pressure and Low Temperature Physics*, C. W. Chu and J. A. Woollam, Eds. (Plenum, New York, 1978), p. 21.
3. D. E. Ramaker, L. Kumar, F. E. Harris, *Phys. Rev. Lett.* **34**, 812 (1975) and references therein.
4. H. K. Mao and P. M. Bell, *Science* **200**, 1145 (1978).
5. R. A. Forman, G. J. Piermarini, J. D. Barnett, S. Block, *ibid.* **176**, 284 (1972).
6. D. E. McCumber and M. D. Sturge, *J. Appl. Phys.* **34**, 1682 (1963).
7. R. A. Noack and W. B. Holzapfel, *High Pressure Science and Technology*, K. D. Timmerhaus and M. S. Barker, Eds. (Plenum, New York, 1979), vol. 1, p. 748.
8. D. H. Liebenberg, R. L. Mills, J. C. Brownson, *Phys. Rev. B* **18**, 4526 (1978).
9. H. K. Mao and P. M. Bell, *Science* **203**, 1004 (1979).
10. The fluorescence of a ruby crystal approximately 20 μm in diameter and having a chromium concentration of 0.55 percent (by weight) was excited by a Liconix helium-cadmium laser. The laser power was varied during the above-mentioned testing by detuning. Because of the long and complicated optical path, the exact laser power received by the ruby crystal is unknown.
11. M. Ross, *J. Chem. Phys.* **60**, 3634 (1974).
12. F. V. Grigorev, S. B. Kormer, O. L. Mikhailova, A. P. Tolochko, V. D. Urlin, *Zh. Eksp. Teor. Fiz.* **69**, 743 (1977) [*Sov. Phys. JETP* **42**, 378 (1976)].
13. We thank H. K. Mao for showing us the construction of a diamond cell and C. Homan for discussion. The work is supported in part by U.S. Army contract DAAA-22-80-C-0101 and the Energy Laboratory of the University of Houston.

4 December 1980; revised 17 March 1981

Uninfected Cells of Soybean Root Nodules: Ultrastructure Suggests Key Role in Ureide Production

Abstract. *In soybean root nodules, which export recently fixed nitrogen mainly as the ureides allantoin and allantoic acid, cells uninfected by rhizobia undergo a pronounced ultrastructural differentiation not shown by the infected cells, including enlargement of the microbodies and proliferation of smooth endoplasmic reticulum. Since some of the enzymes contributing to ureide synthesis occur in these subcellular components in root nodule preparations, the uninfected cells may participate in ureide synthesis and thus play an essential role in the symbiosis between host and bacterium.*

In legume root nodules, the central tissue enclosed by the cortex consists not only of cells that become greatly enlarged and heavily infected with rhizobia but also of many smaller uninfected cells interspersed among the infected ones (*1*). We have found that in soybean (*Glycine max* L.) inoculated with effective strains of *Rhizobium japonicum* (*2*), an ultrastructural differentiation takes place in the uninfected cells which is distinctly different from changes in the infected cells. The principal changes are a marked enlargement of the microbodies and a proliferation of smooth endoplasmic reticulum (ER). We suggest that the ultrastructural responses of the uninfected cells are related to the participation of these cells in metabolic transformations of compounds arising from recently fixed N_2 in the nodule.

Our observations are relevant to current attempts to clarify the major pathway of nitrogen metabolism in soybean root nodules. Legumes are divisible into various groups based on the major nitrogenous compounds transported from the nodules to the shoots. For example, pea (*Pisum*), vetch (*Vicia*), and lupine (*Lupinus*) belong to a group that transports fixed nitrogen mainly as asparagine (*3*). Soybean (*Glycine*), bean (*Phaseolus*), and cowpea (*Vigna*), on the other hand, belong to a group in which the ureides allantoin and allantoic acid are major products of nitrogen assimilation in the nodules (*3–5*) and the principal form of transport of the nitrogen to the shoots (*5, 6*). The rationale for our assumption that the uninfected cells of the soybean nodule are involved in ureide formation depends in part on correla-

0036-8075/81/0619-1394$00.50/0 Copyright © 1981 AAAS